Available online at www.sciencedirect.com
SCIENCE DIRECT®
Journal of Nuclear Materials 328 (2004) 197–214
journal of nuclear materials
www.elsevier.com/locate/jnucmat

Defect production efficiency in metals under neutron irradiation

C.H.M. Broeders [a,*], A.Yu. Konobeyev [a,b]

[a] Forschungszentrum Karlsruhe GmbH, Institut für Reaktorsicherheit, Postfach 3640, Karlsruhe 76021, Germany
[b] Institute of Nuclear and Power Engineering, 249020 Obninsk, Kaluga region, Russia

Received 19 January 2004; accepted 29 April 2004

Abstract

The available data for Frenkel pair resistivity and the experimental data for damage resistivity rate in metals were compiled and analyzed. Based on the data collected the evaluated values of Frenkel pair resistivity for metals have been obtained along with the systematics of the resistivity values. The nuclear data libraries ENDF/B-VI (Release 8), JENDL-3.3, JEFF-3.0, BROND-2.2 and CENDL-2.1 were used for the averaged damage energy cross-section calculation. The defect production efficiency has been calculated with the help of the binary collision approximation model. The values obtained were compared with the result of the molecular dynamics simulation. The energy dependent efficiencies obtained by the method of the molecular dynamics were used for the calculation of the average efficiency values for neutron spectra from various nuclear power facilities including the thermal reactor, the fast breeder reactor and the fusion facility.

1. Introduction

The materials of advanced nuclear power units as the fusion reactor and the accelerator-driven system are considered to be irradiated by extremely fluxes of energetic neutrons and protons. The evaluation of the radiation strength and the accurate calculation of radiation damage take on special significance for materials of these facilities.

The NRT model [1] is frequently used for the calculation of the damage accumulation in irradiated materials. The relative simplicity of the approach provides its use in the popular codes as NJOY [2], MCNPX [3], LAHET [4], SPECTER [5] and others. The available experimental data and more rigorous calculations show the substantial difference with the predictions of the NRT model that makes its use for the reliable calculation of radiation damage rather questionable. However, the previous analysis of the experimental damage rates shown the deviations from the NRT calculation has been performed using the outdated versions of neutron data libraries like as ENDF/B-IV, ENDF/B-V and JENDL-1, which are not in use for applications now. Different authors have used the different sets of Frenkel pair resistivity values and effective threshold energies for the data analysis that complicates the interpretation of the results obtained and the analysis of different irradiation experiments.

The present work is devoted to the analysis of the defect production efficiency in metals irradiated with neutrons of different sources. The available data for Frenkel pair resistivity were compiled and analyzed (Sections 2 and 3). The evaluated and recommended values are presented along with the systematics of Frenkel pair resistivity (Section 3). The available experimental data for damage production rates were collected and examined (Section 4). The damage energy

* Corresponding author. Tel.: +49-7247 82 2484; fax: +49-7247 82 3718/3824.
E-mail address: cornelis.broeders@irs.fzk.de (C.H.M. Broeders).

0022-3115/$ - see front matter © 2004 Published by Elsevier B.V.
doi:10.1016/j.jnucmat.2004.05.002

cross-sections were calculated with the data from ENDF/B-VI (Release 8), JENDL-3.3, JEFF-3.0, BROND-2.2 and CENDL-2.2 for realistic neutron spectra. The average efficiency of the defect production was calculated for different types of the irradiation (Sections 4 and 5).

The MARLOWE code [6] was applied for the calculations of the number of defects in irradiated materials. The results were compared with the simulations performed by the method of the molecular dynamics (Section 5). The theoretical values of the defect production efficiency were applied to the neutron damage calculations for various types of nuclear power facilities, as the thermal reactor, the fast breeder reactor, the fusion reactor and others (Section 5).

2. Efficiency of the defect production in materials

The efficiency of defect production in irradiated materials is defined as follows:

$$\eta = \frac{N_{\mathrm{D}}}{N_{\mathrm{NRT}}}, \tag{1}$$

where N_{D} is the number of stable displacements at the end of collision cascade, and N_{NRT} is the number of defects calculated by the NRT model [1].

In the theoretical simulations based on the method of molecular dynamics (MD) and the binary collision approximation model (BCA) the N_{D} value in Eq. (1) is considered equal to the total number of single interstitial atom–vacancy pairs including the amount in a clustered fraction remaining after the recombination in collision cascade is complete.

The number of defects (Frenkel pair) predicted by the NRT formula [1] is equal to

$$N_{\mathrm{NRT}} = \frac{0.8}{2E_{\mathrm{d}}} T_{\mathrm{dam}}, \tag{2}$$

where E_{d} is the effective threshold displacement energy, and T_{dam} is the 'damage energy' equal to the energy transferred to lattice atoms reduced by the losses for electronic stopping of atoms in displacement cascade.

The effective threshold displacement energy E_{d} in Eq. (2) which is called also as the 'averaged threshold energy' [7,8] is derived from electron irradiation experiments. The compilation of E_{d} values is presented in Section 3. According to other definition [9,10] the value of the effective displacement energy is defined from a condition $\eta = 1$ which relates to a number of defects N_{D} defined from the experiments for neutron irradiation of materials. This effective threshold energy is referred as $E_{\mathrm{d}}(\eta = 1)$ in the present work to separate it from the commonly used effective threshold displacement energy E_{d}.

The average defect production efficiency, $\langle\eta\rangle$ is derived from the experimentally observed resistivity damage rate with the help of the following relation:

$$\left(\frac{\mathrm{d}\Delta\rho}{\mathrm{d}\Phi}\right)\Big|_{\Delta\rho=0} = \langle\eta\rangle\rho_{\mathrm{FP}}\frac{0.8\langle\sigma T_{\mathrm{d}}\rangle}{2E_{\mathrm{d}}}, \tag{3}$$

where $(\mathrm{d}\Delta\rho/\mathrm{d}\Phi)|_{\Delta\rho=0}$ is the initial resistivity-damage rate equal to the ratio of resistivity change $\Delta\rho$ per irradiation fluence Φ extrapolated to zero dose value, ρ_{FP} is the specific Frenkel pair resistivity, $\langle\sigma T_{\mathrm{d}}\rangle$ is the damage energy cross-section averaged for the particle spectrum basing on the NRT model.

The spectrum-averaged damage energy cross-section is calculated as follows:

$$\langle\sigma T_{\mathrm{d}}\rangle = \sum_{i=1}\int\int \varphi(E)\frac{\mathrm{d}\sigma_i(E,T)}{\mathrm{d}T}T_{\mathrm{dam}}(T)\,\mathrm{d}T\,\mathrm{d}E \Big/ \int\varphi(E)\,\mathrm{d}E, \tag{4}$$

where $\mathrm{d}\sigma_i/\mathrm{d}T$ is the spectrum of recoils produced in irradiation of the material with primary particle, $\phi(E)$ is the particle spectrum, T_{dam} is the damage energy calculated according to Ref. [1], the summation is for all channels of the primary particle interaction with material.

The use of Eq. (3) supposes that the resistivity per Frenkel pair does not depend from the degree of defect clusterization in matter and that the resistivity of a cluster is equal to the sum of resistivity of isolated defects. For small clusters it is considered usually as a good approximation [11–14].

According to Eq. (3) the value of defect production efficiency $\langle\eta\rangle$ derived from experimental data depends from the value of Frenkel pair resistivity ρ_{FP} and the effective threshold energy E_{d} adopted for the analysis and from the quality of the $\langle\sigma T_{\mathrm{d}}\rangle$ data. It is the main reason of the considerable scattering of the $\langle\eta\rangle$ values obtained by different authors for the same metals.

3. Resistivity per Frenkel defect and effective threshold displacement energy

3.1. Data compilation and evaluation

Data for the specific Frenkel pair resistivity ρ_{FP} were taken from the papers [9,10,15–68,102–126] relating to the measurements performed after 1962. The reference for the early measurements for copper, silver and gold can be found in Refs. [34,41].

Data for Frenkel pair resistivity were subdivided in several groups by the method of their derivation: the data obtained by the X-ray diffraction method, the data extracted from the electron irradiation of single crystals

at low temperature, the ρ_{FP} values obtained from the experiments with polycrystals, the data evaluated by the analysis of various experiments and the data obtained with the help of systematics. If the detailed information about the method of data derivation is absent, the data are referred as 'adopted' by the authors of a certain work.

The collected values of ρ_{FP} are shown in Table 1. The data are presented for the metals with face-centered cubic lattice (*fcc*) at first, than for the body-centered cubic metals (*bcc*), for the metals with hexagonal lattice (*hcp*) and for other metals.

The evaluation of Frenkel pair resistivity for each element from Table 1 was performed by the statistical analysis taking into account the relative accuracy of the method of data derivation and the experimental errors. If only systematics data are available for a certain metal the recommended value of ρ_{FP} is not given. The evaluated values of Frenkel pair resistivity are shown in Table 1 (sixth column).

The adopted values of ρ_{FP} are slightly different from ones obtained in Ref. [102]. Mainly, it results from the different principles of the evaluation in Ref. [102] and in the present work. As a rule, the ρ_{FP} value for a certain element recommended in Ref. [102] corresponds to a single reliable measurement. In the present work the results of the different most reliable measurements were analyzed statistically.

The effective threshold displacement energies E_d taken from literature are shown in Table 1. If the same E_d value was used by different authors only the single reference is given. Also, the adopted E_d values used in the present work for damage production efficiency calculations are shown in Table 1 (ninth column).

It should be noted that the exact absolute values of threshold energy E_d is of secondary importance in the case the experimental dose rates are known. They are used only for the comparison of defect production efficiency in different experiments.

3.2. Systematics of Frenkel pair resistivity

The evaluated and adopted values of Frenkel pair resistivity (Table 1) were used to constrain the systematics of ρ_{FP} by the method proposed by Jung [18]. The systematics combines the Frenkel pair resistivity, the resistivity at the melting point and the bulk modulus of the material. The general form of the systematics is as follows [18]:

$$\rho_{FP} = \rho(T_{melt})(\alpha_1 + \alpha_2(B\Omega)^{\alpha_3}), \quad (5)$$

where $\rho(T_{melt})$ is the resistivity at the melting temperature, B is the bulk modulus, Ω is the atomic volume, and α_i are the parameters to be obtained by the fitting procedure.

The experimental values of the resistivity at the melting point $\rho(T_{melt})$ were taken from Ref. [69]. If absent, the $\rho(T_{melt})$ values were taken from Ref. [18] or evaluated with the help of the following approximate formula [70]:

$$\rho(T_{melt}) = \rho(T_0)\frac{T_{melt}}{T_0}\frac{F(\theta/T_{melt})}{F(\theta/T_0)}, \quad (6)$$

where $\rho(T_0)$ is the resistivity at the temperature T_0, θ is the Debye temperature and F is the universal function.

The values of $F(x)$ function are tabulated in Ref. [70] and can be approximated with a good accuracy at $x \leqslant 6$ by the following formula:

$$F(x) = 2.884 \times 10^5 (55.5 + x^{1.98})^{-3.13}. \quad (7)$$

Data for the resistivity $\rho(T_0)$ were taken from Ref. [69] at $T_0 = 293$–300 K, the Debye temperature and the bulk modulus are from Ref. [71]. The atomic volume Ω was calculated as the inverse of the atomic concentration.

The fitting of Eq. (5) to the adopted values of ρ_{FP} from Table 1 gives the following systematics of Frenkel pair resistivity:

$$\rho_{FP} = \rho(T_{melt})\left(8.03 + 40.51(B\Omega)^{-1.532}\right), \quad (8)$$

where the product $B\Omega$ is taken in the units 10^{-18} N m.

Below, the systematics Eq. (8) is used for the ρ_{FP} value evaluation if the experimental data are absent.

The ratio $\rho_{FP}/\rho(T_{melt})$ predicted by the systematics Eq. (8) is shown for various metals in Fig. 1.

4. Average efficiency of defect production derived from experimental damage rates for materials irradiated at low temperature (4–5 K)

The experimental damage resistivity rates were taken from Refs. [7,12,31,38,43,47,63,65,72–75]. The data are shown in Table 2 for various metals and types of irradiation.

If the detail information about the neutron irradiation spectrum was available, the averaged damage energy cross-section $\langle \sigma T_d \rangle$ was calculated and checked in the present work.

The NJOY code system [2] has been applied for the damage energy cross-section calculation. The calculations were performed with the data taken from ENDF/B (different versions), JENDL-3.3 and JEFF-3.0 for the temperature of materials at 4–5 K. The additional calculations show that the influence of the temperature on the averaged $\langle T_d \rangle$ values is rather weak.

Below the values of the averaged damage energy cross-sections used for the analysis of the damage production efficiency in Section 4.2 are discussed for the different types of irradiation.

Table 1
The Frenkel pair resistivity ρ_{FP} and the effective threshold displacement energy E_d taken from literature and the values of ρ_{FP} and E_d evaluated and adopted for the analysis of the defect production efficiency. Methods of the data derivation: 'Exp D' is X-ray diffraction method, 'Exp T' is the threshold energy determination for electron irradiation of single crystals at low temperature, 'Exp T(p)' is for the electron irradiation of polycrystals, 'Evl E' is the evaluation performed basing on the analysis of different experiments, 'Evl S' is the estimation made with the help of the systematics, 'Adp' is the data adopted by the authors of cited works

Metal	Lattice	ρ_{FP} ($\mu\Omega$ m)	Type	Reference	Adopted ρ_{FP} ($\mu\Omega$ m)	E_d (eV)	Reference	Adopted E_d (eV)
13 Al	fcc	3.9 ± 0.6	Exp D	[15]	3.7	27	[22]	27
		4.2 ± 0.8	Exp D	[16]		45	[23]	
		3.2 ± 0.6	Exp D	[17]		66	[9]	
		3.4	Exp T(p)	[33]				
		1.4...4.4	Exp T(p)	[102,103]				
		1.32	Exp T(p)	[104]				
		1.35	Exp T(p)	[102,105]				
		4.0	Evl E	[22,102]				
		4.0 ± 0.6	Evl E	[10,18]				
		4.2 ± 0.5	Evl E	[19]				
		6.8	Adp	[20]				
		4.3	Evl S	[18]				
28 Ni	fcc	7.1 ± 0.8	Exp D	[24]	7.1	33	[22]	33
		3.2	Exp T(p)	[33]		40	[25]	
		6.7 ± 0.4	Evl E	[19]		69	[9]	
		6.0	Adp	[38]				
		6.4	Adp	[20]				
		11.2	Evl S	[18]				
29 Cu	fcc	1.7 ± 0.3	Exp T	[26]	2.2	25	[29]	30
		2.0 ± 0.4	Exp D	[27]		29	[22]	
		2.2 ± 0.5	Exp D	[106]		30	[14]	
		$2.75^{+0.6}_{-0.2}$	Exp T	[28]		43 ± 4	[9]	
		2.5 ± 0.3	Exp D	[102]				
		1.3	Exp T(p)	[33]				
		1.15...2.06	Exp T(p)	[102,103]				
		1.9 ± 0.2	Evl E	[19]				
		2.2	Evl E	[31]				
		3.0	Evl E	[34]				
		2.5	Adp	[20]				
		2.2	Evl S	[18]				
46 Pd	fcc	9.0 ± 1.0	Exp T(p)	[32]	9.0	34	[32]	41
		10.5	Adp	[9]		41	[22]	
		9.2 ± 0.5	Evl S	[19]		46	[9]	
		9.0	Evl S	[18]				
47 Ag	fcc	1.4	Exp T(p)	[33]	2.1	39	[22]	39
		2.5	Adp	[20]		44	[9]	
		2.1 ± 0.4	Evl S	[19]		60	[30]	
		2.1	Evl S	[10]				
		1.8	Evl S	[18]				
77 Ir	fcc	6.7 ± 0.5	Exp T(p)	[122]	6.7			
78 Pt	fcc	9.5 ± 0.3	Exp T	[26]	9.5	43	[25]	44
		7.5	Exp T(p)	[35]		44	[22]	
		6.0	Exp T(p)	[40]		44 ± 5	[9]	
		9.5 ± 0.5	Evl E	[19]				
		7.0	Adp	[31]				
		9.5	Evl S	[18]				

Table 1 (*continued*)

Metal	Lattice	ρ_{FP} (μΩm)	Type	Reference	Adopted ρ_{FP} (μΩm)	E_d (eV)	Reference	Adopted E_d (eV)
79 Au	fcc	1.2	Exp T	[36]	2.6	30	[30]	43
		3.2 ± 0.3	Exp D	[37]		35	[29]	
		0.89	Exp T(p)	[39]	43	[22]		
		5.1 ± 0.3	Evl S	[19]		44	[9]	
		2.3	Evl S	[18]				
		2.5	Adp	[20]				
82 Pb	fcc	>1	Exp T(p)	[107]	–	19	[7]	25
		16.4	Evl S	[18]		25	[30]	
		20.0	Adp	[22,102]				
90 Th	fcc	15	Exp T(p)	[102]	19			
		19	Evl E	[22,102]				
		18.6	Evl S	[18]				
23 V	bcc	6 + 1.52 −0.84	Exp T(p)	[108]	21	40	[30]	57
		22.0 ± 7.0	Evl S	[19]		57	[43]	
		18.0	Adp	[38]		92	[9]	
		23	Adp	[9]				
		40	Evl S	[50]				
		21.6	Evl S	[18]				
		22	Evl S	[10]				
		16	Evl S	[42]				
24 Cr	bcc	37 + 2 −12	Exp T	[109]	37	40	[30]	40
		40	Exp T(p)	[109,110]				
		27.1	Evl S	[18]				
		30.0	Evl S	[49]				
26 Fe	bcc	30 ± 5.0	Exp T	[44]	24.6	24	[45]	40
		20	Exp D	[46]		25	[29]	
		12.5	Exp T(p)	[33]		40	[30]	
		15	Adp	[22,47]		44	[22]	
		17 ± 6	Evl S	[19]				
		25.2	Evl S	[18]				
		19	Adp	[49]				
41 Nb	bcc	14.0 ± 3.0	Exp D	[48]	14	40	[30]	78
		14.0 ± 3.0	Evl E	[19]		78	[22]	
		16.0	Evl S	[10]		98	[9]	
		15.4	Evl S	[18]				
		27.0	Evl S	[49]				
		18.0	Adp	[9]				
		10.0	Adp	[42]				
42 Mo	bcc	13 ± 2.0	Exp T	[51]	13.4	33	[54]	65
		15 ± 4.0	Exp D	[52]		60	[30]	
		4.5	Exp T(p)	[33]		60–70	[22]	
		15 ± 4	Evl E	[19]		70	[43]	
		15 ± 5	Evl E	[18]		77	[47]	
		14 ± 3	Evl E	[53]		82	[9]	
		13.2	Evl S	[18]				
		14	Evl S	[10]				
		10	Evl S	[21,50,111]				
73 Ta	bcc	17 ± 3	Exp T	[55]	16.5	85	[43]	90
		16 ± 3	Exp T	[56]		80–90	[22]	

(*continued on next page*)

Table 1 (*continued*)

Metal	Lattice	ρ_{FP} ($\mu\Omega$ m)	Type	Reference	Adopted ρ_{FP} ($\mu\Omega$ m)	E_d (eV)	Reference	Adopted E_d (eV)
		16 ± 3	Evl E	[19]		88	[9]	
		17.8	Evl S	[18]		90	[30]	
74	W bcc	7.5...16	Exp T	[102,112]	27	84	[57,65]	90
		28	Exp T(p)	[102,113]		90	[30]	
		27 ± 6	Evl S	[19]		100	[43]	
		18	Evl S	[10]				
		18.3	Evl S	[18]				
		13	Evl S	[49]				
		14	Adp	[57]				
12 Mg	hcp	9.0	Exp D	[66]	9	20	[22]	20
		$\geqslant 0.8$	Exp T(p)	[102,114]		25	[30]	
		4.5	Exp T(p)	[58]				
		4.0	Evl E	[22,102]				
		21.5	Evl S	[18]				
		4.0	Adp	[22,52]				
21 Sc	hcp	50.0	Exp T(p)	[124]	50.0			
22 Ti	hcp	18.0	Exp T(p)	[59]	24.9	30	[22]	30
		42.0	Exp T(p)	[33]		40	[30]	
		32.3	Evl S	[18]				
		22.0	Evl S	[43]				
		10.0	Adp	[22,43]				
27 Co	hcp	$30 + 20$ -10	Exp T	[61]	15.5	36	[22]	36
		15 ± 5	Exp T	[60]		40	[30]	
		16 ± 5	Exp D	[66]				
		14 ± 4	Evl E	[19]				
		18.4	Evl S	[18]				
		20.0	Evl S	[50]				
		10.0	Evl S	[21]				
30 Zn	hcp	15 ± 5	Exp T	[60]	17.9	29	[22]	29
		15 ± 5	Exp D	[52]				
		15.3	Exp D	[62]				
		20 ± 3	Exp T	[61]				
		4.2 ± 0.5	Exp T(p)	[116]				
		15.1	Evl S	[18]				
		5	Adp	[115]				
		10	Adp	[22,52]				
39 Y	hcp	50 ± 20	Exp T(p)	[125]	50			
40 Zr	hcp	35 ± 8	Exp D	[66]	37.5	40	[22]	40
		40	Exp(p)	[67]				
		35 ± 8	Evl E	[19]				
		30.1	Evl S	[18]				
		40	Adp	[22,43]				
48 Cd	hcp	5 ± 1	Exp T	[61]	14.5	30	[22]	30
		10	Exp D	[66]				
		19 ± 8	Evl S	[19]				
		10.9	Evl S	[18]				
		10	Adp	[52]				
59 Pr	hcp	135 ± 35	Exp T(p)	[123]	135			
60 Nd	hcp	135 ± 35	Exp T(p)	[123]	135			
63 Eu	hcp	$\geqslant 100$	Exp T(p)	[121]	–			

Table 1 (*continued*)

Metal	Lattice	ρ_{FP} (μΩm)	Type	Reference	Adopted ρ_{FP} (μΩm)	E_d (eV)	Reference	Adopted E_d (eV)
64 Gd	hcp	160 ± 30	Exp T(p)	[118]	160			
65 Tb	hcp	155 ± 30	Exp T(p)	[118]	155			
66 Dy	hcp	145 ± 30	Exp T(p)	[118]	145			
67 Ho	hcp	145 ± 30	Exp T(p)	[118]	145			
68 Er	hcp	180 ± 35	Exp T(p)	[118]	180			
69 Tm	hcp	140 ± 30	Exp T(p)	[118]	140			
70 Yb	hcp	75 ± 25	Exp T(p)	[125]	75			
71 Lu	hcp	75 ± 15	Exp T(p)	[117]	145			
		145 ± 30	Exp T(p)	[118]				
		81.0	Evl S	[18]				
75 Re	hcp	20	Exp T(p)	[119]	20	60	[22]	60
		22	Evl S	[18]				
		20	Adp	[22,63]				
31 Ga	bco[a]	5.4 ± 0.5	Exp T(p)	[64]	5.4	12	[64]	12
92 U	bco	22	Exp T	[126]	22			
49 In	bct[b]	2.6	Exp T(p)	[107]	2.6			
50 ßSn	bct	1.1 ± 0.2	Exp T(p)	[68]	1.13	22	[68]	22
		4 ± 2	Evl S	[19]				
62 Sm	rho[c]	140 ± 30	Exp T(p)	[125]	140			
83 Bi	rho	7500 ± 2000	Exp T(p)	[120]	–			
	SS[d]	25	Adp	[10]	25			40

[a] Base-centered orthorhombic lattice.
[b] Body-centered tetragonal lattice.
[c] Rhombohedral lattice.
[d] Stainless steel, the composition is not shown [10].

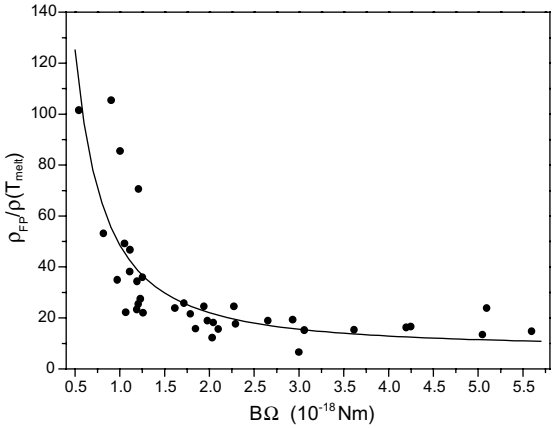

Fig. 1. The ratio of the Frenkel pair resistivity to the resistivity at the melting point versus $B\Omega$ for various metals (full circles) and the systematics prediction (line).

4.1. Averaged damage energy cross-sections

Data are discussed for various neutron sources listed below.

4.1.1. CP-5 (VT53), ANL

The $\langle \sigma T_d \rangle$ data shown in Table 2 are taken mainly from Ref. [47].

4.1.2. LTIF, ORNL

Data for Al, Cu, Pt, V, Nb and Mo were obtained by the averaging-out the $\langle \sigma T_d \rangle$ values from Refs. [43,65].

The $\langle \sigma T_d \rangle$ value for the stainless steel (15 Cr/15 Ni/70 Fe) has been calculated approximately. The averaged damage energy cross-section was calculated with the data from ENDF/B-VI (Release 8) for various elements from Ref. [43] for the fission neutron spectrum. The mean ratio of the $\langle \sigma T_d \rangle$ values obtained in Ref. [43] for LTIF spectrum to the $\langle \sigma T_d \rangle$ values calculated for the fission spectrum was found equal to 1.147. This ratio

Table 2
Low temperature damage-resistivity rate $(d\Delta\rho/d\Phi)|_{\Delta\rho=0}$, the averaged damage energy cross-section $\langle\sigma T_d\rangle$, the defect production efficiency and the effective threshold displacement energy $E_d(\eta = 1)$

Metal	Source	$(d\Delta\rho/d\Phi)\|_{\Delta\rho=0}$ (10^{-31} Ω m^3)	$\langle\sigma T_d\rangle$ (b keV)	Reference	Efficiency	$E_d(\eta = 1)$ (eV)
fcc metals						
Al	CP-5 (VT53), ANL	1.49	76.2	[47]	0.357	75.7
Al	FISS FRAGM	57.6	2492	[47,72][a]	0.422	64.0
Al	LTIF, ORNL	2.19	98.55	[43,38,65]	0.405	66.6
Al	RTNS, LLL	4.18	156.9	[65]	0.486	55.6
Al	LHTL, JPR-3	2.20	81.0	[63]	0.495	54.5
Al	TTB(1), FRM	2.57	87.6	[7]	0.535	50.4
Ni	CP-5 (VT53), ANL	1.14	59.0	[47]	0.225	147.0
Ni	FISS FRAGM	48.0	3400	[47,72][a]	0.164	201.2
Ni	LTIF, ORNL	1.71	85.4	[43,38]	0.233	141.8
Ni	LHTL, JPR-3	2.3	83.2	[63]	0.321	102.7
Ni	TTB(2), FRM	1.86	76.05	[7,31]	0.284	116.1
Cu	CP-5 (VT53), ANL	0.424	56.3	[47]	0.257	116.8
Cu	FISS FRAGM	30.0	3295	[47,72][a]	0.310	96.7
Cu	HEAVY IONS			[47,12]	0.333	90.1
Cu	Be(40MeV-d,n)	2.11	233.4	[47,65]	0.308	97.3
Cu	LTIF, ORNL	0.723	81.7	[43,38,65]	0.302	99.4
Cu	RTNS, LLL	2.48	288.5	[65]	0.293	102.4
Cu	LHTL, JPR-3	0.70	81.6	[63]	0.292	102.6
Cu	TTB(1), FRM	0.71	68.9	[7]	0.351	85.4
Pd	LTIF, ORNL	1.90	73	[43,38]	0.296	138.3
Pd	TTB(2), FRM	1.78	59.41	[7,31]	0.341	120.2
Ag	CP-5 (VT53), ANL	0.295	47.3	[47]	0.290	134.7
Ag	FISS FRAGM	13.8	4004	[47,72][a]	0.160	243.7
Ag	HEAVY IONS			[47,12]	0.400	97.5
Ag	LTIF, ORNL	0.666	72	[43]	0.429	90.8
Ag	LHTL, JPR-3	0.70	71.7	[63]	0.453	86.0
Ag	TTB(1), FRM	0.70	76.4	[7]	0.425	91.7
Pt	CP-5 (VT53), ANL	0.818	32.4	[47]	0.292	150.5
Pt	Be(40MeV-d,n)	4.72	175	[47,65]	0.312	140.9
Pt	LTIF, ORNL	1.59	48.4	[43,65]	0.380	115.7
Pt	LHTL, JPR-3	1.7	48.8	[63]	0.403	109.1
Pt	TTB(1), FRM	1.56	40.55	[7]	0.445	98.8
Au	LHTL, JPR-3	0.5	50.2	[63]	0.412	104.4
Au	TTB(2), FRM	0.61	55.78	[7,31]	0.452	95.1
Pb	TTB(2), FRM	1.3	46.68	[7,73]	0.101[b]	247.0
bcc metals						
K	TTB(2), FRM	1.56	71.68	[7,75]	0.065[c]	619.4
V[d]	LTIF, ORNL	7.17	98.05	[43,38,65]	0.496	114.9
V	RTNS, LLL	18.01	257.1	[65]	0.475	119.9
V	LPTR(FNIF-10)	6.56	79.2	[65]	0.562	101.4
V	Be(30 MeV-d,n)	14.03	200	[65]	0.476	119.7
V	LHTL, JPR-3	8.0	98.5	[63]	0.551	103.4
V	TTB(2), FRM	7.3	90.78	[7,73]	0.546	104.5
Fe	CP-5 (VT53), ANL	3.33	50.7	[47]	0.267	149.8
Fe	LHTL, JPR-3	6.5	84.6	[63]	0.312	128.1
Fe	TTB(1), FRM	6.39	70.9	[7]	0.366	109.2
Nb	CP-5 (VT53), ANL	2.19	55.7	[47]	0.548	142.4
Nb[d]	LTIF, ORNL	3.43	80.25	[43,38,65]	0.595	131.0

Table 2 (*continued*)

Metal	Source	$(d\Delta\rho/d\Phi)\|_{\Delta\rho=0}$ (10^{-31} Ω m^3)	$\langle\sigma T_d\rangle$ (b keV)	Reference	Efficiency	$E_d(\eta=1)$ (eV)
Nb	Be(30 MeV-d,n)	7.38	197	[65]	0.522	149.5
Nb	Be(40 MeV-d,n)	10.1	223.9	[47,65]	0.628	124.1
Nb	LPTR(FNIF-10)	3.47	60.3	[65]	0.802	97.3
Nb	RTNS, LLL	11.44	283.3	[65]	0.562	138.7
Nb	LHTL, JPR-3	6.5	80.2	[63]	1.129	69.1
Nb	TTB(2), FRM	2.7	68.8	[7,73]	0.547	142.7
Mo	(CP-5 VT53), ANL	1.86	61.2	[47]	0.369	176.4
Mo[d]	LTIF, ORNL	3.38	84.55	[43,38,65]	0.485	134.1
Mo	Be(30 MeV-d,n)	6.10	192	[65]	0.385	168.7
Mo	LPTR(FNIF-10)	3.00	69.5	[65]	0.523	124.2
Mo	RTNS, LLL	9.47	253.5	[65]	0.453	143.5
Mo	LHTL, JPR-3	3.2	69.6	[63]	0.558	116.6
Mo	TTB(1), FRM	3.34	76.3	[7]	0.531	122.4
Ta	LTIF, ORNL	2.52	54.7	[43]	0.628	143.3
Ta	LHTL, JPR-3	3.2	55.7	[63]	0.783	114.9
Ta	TTB(1), FRM	2.51	44.3	[7]	0.773	116.5
W[e]	LTIF, ORNL	4.2	52.2	[43]	0.670	134.2
W	RTNS, LLL	11.55	195.1	[65]	0.493	182.4
W	LHTL, JPR-3	3.9	51.3	[63]	0.634	142.1
W	TTB(1), FRM	3.3	42.8	[7]	0.643	140.1
hcp metals						
Mg	LTIF, ORNL	7.0	92.7	[43]	0.420	47.7
Mg	LHTL, JPR-3	6.5	75.2	[63]	0.480	41.6
Ti	LTIF, ORNL	22.4	97.6	[43]	0.691	43.4
Ti	LHTL, JPR-3	35.0	94.9	[63]	1.111	27.0
Ti	TTB(1), FRM	21.6	80.8	[7]	0.805	37.3
Co	CP-5 (VT53), ANL	2.42	56.0	[47]	0.251	143.5
Co	LHTL, JPR-3	4.9	85.0	[63]	0.335	107.6
Co	TTB(1), FRM	3.27	86.6	[7]	0.219	164.2
Zn	LHTL, JPR-3	8.0	87.9	[63]	0.369	78.7
Zr	LTIF, ORNL	24.0	74.8	[43]	0.856	46.8
Zr	LHTL, JPR-3	23.0	84.6	[63]	0.725	55.2
Zr	TTB(1), FRM	16.5	75.0	[7]	0.587	68.2
Cd	LHTL, JPR-3	5.8	67.1	[63]	0.447	67.1
Gd	LHTL, JPR-3	13.0	52.51	[63]	0.155[f]	258.5
Re	LHTL, JPR-3	6.0	51.61	[63]	0.872	68.8
Other metals						
Ga	LHTL, JPR-3	13.0	79.57	[63]	0.908	13.2
Sn	TTB(2), FRM	1.12	69.07	[7,74]	0.789	27.9
SS	LTIF, ORNL	6.37	86.73	[38]	0.294	136.2

[a] The $\langle\sigma T_d\rangle$ value is calculated formally using the data from Tables 6 and 4 of [47].

[b] Pb: $\rho_{FP} = 17.2$ μΩ m, Eq. (8); $E_d = 25$ eV.

[c] K: $\rho_{FP} = 33.7$ μΩ m, Eq. (8); $E_d = 40$ eV.

[d] Material is doped with 300 ppm Zr.

[e] High level of impurities and cold-worked conditions for the measurement for tungsten were noted in [43]. The possible error for damage rate was estimated as 20–50% [43].

[f] Gd: $E_d = 40$ eV.

was used for the evaluation of the $\langle \sigma T_d \rangle$ value for stainless steel irradiated with neutrons with the LTIF spectrum basing on the calculations performed for Cr, Fe and Ni for the fission neutron spectrum.

4.1.3. RTNS, LLL

The values of $\langle \sigma T_d \rangle$ shown in Table 2 were obtained using the ENDF/B-VI(8) data at the neutron energy equal to 14.8 MeV. The data are close to ones taken from JENDL-3.3 and from Ref. [65].

The mean deviation of the $\langle \sigma T_d \rangle$ values from JENDL-3.3 and ENDF/B-VI(8) defined as

$$(100/N)\sum_{i=1}^{N} \left| \langle \sigma T_d \rangle_2 - \langle \sigma T_d \rangle_1 \right| / \langle \sigma T_d \rangle_2$$

is equal to 4.7%; for the values from Ref. [65] and ENDF/B-VI(8) – 5.2%.

4.1.4. Be(d,n)

For the Be(d,n) reaction induced by the 40-MeV deuterons the $\langle T_d \rangle$ values were calculated with the neutron spectrum from Ref. [47] and the ENDF/B-VI(8) data which are available at the energies covering the spectrum of the Be(d,n) reaction.

The $\langle \sigma T_d \rangle$ value for platinum was calculated approximately. Data for 38 nuclides from ^{27}Al to ^{209}Bi from ENDF/B-VI(8) at the energies up to 30 or 150 MeV were used to obtain the contribution of the energy range below 20 MeV in the total averaged damage energy cross-section. Fig. 2(a) shows the relative value of this contribution equal to $\langle \sigma T_d \rangle (E < 20 \text{ MeV}) / \langle \sigma T_d \rangle (\text{total})$ and the approximation curve. The value of $\langle \sigma T_d \rangle (E < 20 \text{ MeV})$ for platinum has been calculated with the data from JEFF-3.0 (ENDL-78). Basing on the simple approximation for the obtained ratio $\langle \sigma T_d \rangle (E < 20 \text{ MeV}) / \langle \sigma T_d \rangle (\text{total})$, the total $\langle \sigma T_d \rangle$ value for platinum has been estimated (Fig. 2(b)). This value equal to 175 b keV is shown in Table 2. It should be noted that the authors of Ref. [65] have used the $\langle \sigma T_d \rangle$ value equal to 182 b keV and the authors of Ref. [47] – 198 b keV.

The $\langle \sigma T_d \rangle$ values for 30-MeV deuteron irradiation of V, Nb and Mo were taken from Ref. [65].

4.1.5. LHTL, JPR-3

The radiation damage rates for materials irradiated in the LHTL facility have been measured in Ref. [63]. The $\langle \sigma T_d \rangle$ cross-sections have been calculated by the authors [63] for the fission neutron spectrum with the ENDF/B-IV and JENDL-1 data.

Unfortunately, the detail description of irradiation neutron spectrum is absent in Ref. [63]. The calculation performed in the present work with the ENDF/B-IV data for different types of fission neutron spectrum does not reproduce the $\langle \sigma T_d \rangle$ values from Ref. [63] precisely. The difference in the $\langle \sigma T_d \rangle$ values may result as from the shapes of fission neutron spectra as from the methods of the $\langle \sigma T_d \rangle$ calculation.

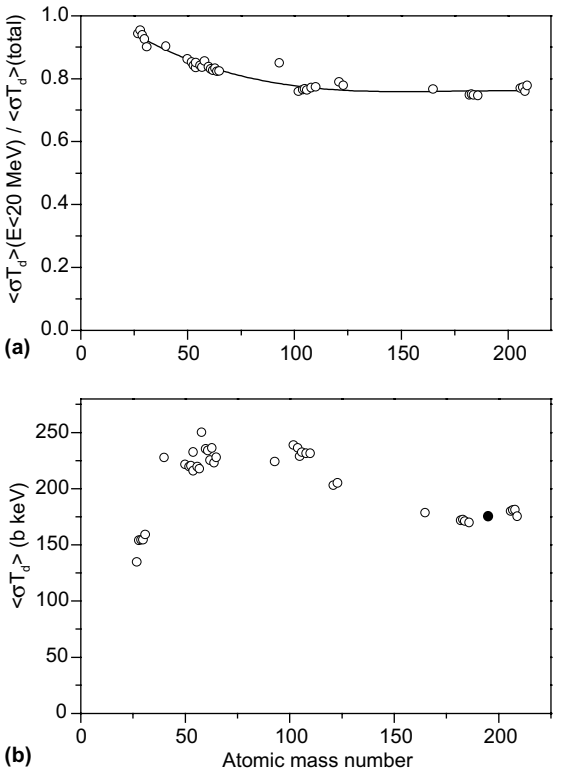

Fig. 2. (a) The relative contribution of the energies below 20 MeV in the total averaged damage energy cross-section for the Be(d,n) spectrum calculated with the data from ENDF/B-VI(8) (circle) and the approximation curve. (b) The total averaged damage energy cross-sections for Be(d,n) spectrum calculated for different nuclides (open circles) and the value evaluated for platinum (full circle).

Fig. 3 shows the $\langle \sigma T_d \rangle$ values from Ref. [63] and the cross-sections calculated in the present work for elements with atomic number from 11 to 83 and nuclear data from ENDF/B-VI(8) and from JENDL-3.3. The calculations are performed for the Maxwellian fission neutron spectrum with $\theta = 1.318$ MeV which provide the best description of the $\langle \sigma T_d \rangle$ values from Ref. [63] integrally. The noticeable difference in the $\langle T_d \rangle$ values obtained in Ref. [63] and in the present work is for the light elements (Al, Mg) and for Mo. The mean deviation of the $\langle \sigma T_d \rangle$ values from Ref. [63] and the cross-sections obtained here with the data from ENDF/B-VI(8) is equal to 6.6%, with the data from ENDF/B-IV – 7.6%. At the same time the deviation of the $\langle \sigma T_d \rangle$ values obtained in the present work using the ENDF/B-IV data and the ENDF/B-VI(8) data is equal to 3.2% for metals investigated in Ref. [63]. The most difference in ENDF/B-IV and ENDF/B-VI(8) based $\langle \sigma T_d \rangle$ calculations is for cadmium (22%).

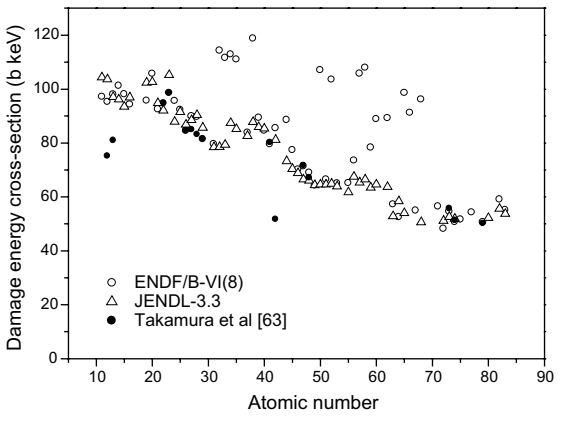

Fig. 3. The averaged damage energy cross-section for natural mixtures of isotopes with atomic numbers from 11 to 83 calculated with the help of the NJOY code for fission neutron spectrum using the data from ENDF/B-VI(8) (open circles) and JENDL-3.3 (triangles) and the values calculated in Ref. [63] with the data taken from ENDF/B-IV (full circles).

For platinum the $\langle \sigma T_d \rangle$ value shown in Table 2 has been obtained using the data from JEFF-3.0 and Maxwellian spectrum with $\theta = 1.318$ MeV. The use of the fission spectrum with $\theta = 1.375$ MeV gives the $\langle \sigma T_d \rangle$ value equal to 50.3 b keV and the use of the combined fission spectrum from Ref. [76] – 42.7 b keV.

The averaged damage energy cross-section for molybdenum was obtained by the averaging-out of the $\langle \sigma T_d \rangle$ values data from Ref. [63] obtained with the data from different data libraries.

For zinc the averaged $\langle \sigma T_d \rangle$ value was evaluated using the data from CENDL-2.1 (90.6 b keV) and JEFF-3.0 (BROND-2.2) (85.2 b keV). The $\langle \sigma T_d \rangle$ value for zirconium was obtained using ENDF/B-VI(8) and the same fission neutron spectrum with $\theta = 1.318$ MeV.

For gadolinium the average damage energy cross-section was obtained with the help of the data taken from different origins. Table 2 shows the $\langle \sigma T_d \rangle$ value equal to 52.51 b keV calculated with the ENDF/B-VI(8) data. The use of the data from JENDL-3.3 gives 58.37 b keV, JEFF-3.0 – 76.72 b keV and BROND-2.2 – 59.54 b keV for the Maxwellian spectrum with equal to 1.318 MeV. It should be noted that the $\langle \sigma T_d \rangle$ value for gadolinium is rather sensitive to the shape of the neutron spectrum at low energies. Mainly, it originates from the anomalous high radiative capture cross-section for ^{155}Gd and ^{157}Gd isotopes at the energies below 10 eV. The calculation with the fission spectrum from Ref. [76] gives the $\langle \sigma T_d \rangle$ values, which are highly different from the ones mentioned above: ENDF/B-VI(8) – 283.4 b keV, JENDL-3.3 – 288.7 b keV, JEFF-3.0 – 255.2 b keV, BROND-2.2 – 289.5 b keV (weighted sum for individual isotopes). In all cases the effective threshold displacement energy was taken equal to 40 eV for gadolinium.

Table 2 shows the $\langle \sigma T_d \rangle$ value for rhenium obtained with the help of the data from ENDF/B-VI(8). This value is close to $\langle \sigma T_d \rangle$ calculated with the data from BROND-2.2 which is equal to 48.09 b keV.

For gallium the calculation with the data from ENDF/B-VI(8) gives 79.57 b keV (Table 2) and with the data from JENDL-3.3 – 78.48 b keV.

4.1.6. TTB, FRM

Data for the TTB neutron spectrum (Figs. 6 and 7) are subdivided on two groups in Table 2. The first group (TTB(1)) contains the $(d\Delta\rho/d\Phi)|_{\Delta\rho=0}$ rates and the $\langle \sigma T_d \rangle$ values obtained in Ref. [7] for the measured neutron spectrum. The second group (TTB(2)) includes data for $(d\Delta\rho/d\Phi)|_{\Delta\rho=0}$ obtained in Refs. [31,73–75] for modified TTB spectrum and corrected as described in Ref. [7].

In the present work the $\langle \sigma T_d \rangle$ values were calculated for the TTB spectrum measured in Ref. [7] and tabulated in Ref. [77]. Table 3 shows the average damage energy cross-sections calculated with the help of the SPECTER code in Ref. [77] and with the help of the NJOY code with the data from ENDF/B-V, ENDF/B-VI(8) and JENDL-3.3 for a number of metals examined in Ref. [7]. The calculations by the SPECTER code [77] are based mainly on the ENDF/B-V data.

There is a good agreement in $\langle \sigma T_d \rangle$ values obtained by the different tools and data libraries. The mean deviation of the averaged cross-sections obtained with the help of the SPECTER code and the NJOY code with the data from ENDF/B-V is equal to 2.2%, for the NJOY calculation with the data from ENDF/B-V and ENDF/B-VI(8) – 1.9%, for the NJOY calculation with the data from JENDL-3.3 and ENDF/B-VI(8) – 5.0%.

The values of $\langle \sigma T_d \rangle$ calculated by the SPECTER code were used in Ref. [7] for the analysis of the defect production efficiency. The measured $(d\Delta\rho/d\Phi)|_{\Delta\rho=0}$ values were scaled in Ref. [7] according to the neutron flux contribution above 0.1 MeV. The corresponding change was done for the averaged damage energy cross-sections, which explains the main difference in the $\langle \sigma T_d \rangle$ values shown in Tables 2 and 3.

The $\langle \sigma T_d \rangle$ values shown in Table 2 for palladium (59.41 b keV) and lead (46.68 b keV) were obtained with the neutron data from ENDF/B-VI(8). The corresponding values calculated with the data from JENDL-3.3 are 59.82 b keV and 44.28 b keV. For tin the averaged value equal to 69.07 b keV obtained with the help of ENDF/B-VI(8) (85.75 b keV) and JENDL-3.3 (52.39 b keV) is shown.

The calculation of the $\langle \sigma T_d \rangle$ value for platinum has been performed with the data from JEFF-3.0 (ENDL-78).

4.2. Defect production efficiency

The calculated values of defect production efficiency $\langle \eta \rangle$ and the effective threshold displacement energy

Table 3
The averaged damage energy cross-section (b keV) for TTB neutron spectrum [7] calculated with the help of the SPECTER code [77] and the NJOY code with the data from ENDF/B-V, ENDF/B-VI(8) and JENDL-3.3

Metal	SPECTER [77]	NJOY		
		ENDF/B-V	ENDF/B-VI(8)	JENDL-3.3
Al	26.39	26.98	26.94	27.02
K	21.56	22.99	23.01	24.26
Ti	24.22	24.71	24.65	24.86
V	27.45	27.55	27.25	28.61
Fe	21.36	21.48	21.44	21.95
Co	26.03	26.29	26.99	26.16
Ni	22.87	23.74	23.95	24.08
Cu	20.76	20.59	21.33	22.28
Zr	22.64	22.43	22.41	22.11
Nb	20.80	21.00	20.77	18.78
Mo	23.11	23.04	22.35	21.17
Ag	24.16	25.35	25.35	18.33
Ta	13.86	13.72	13.72	13.66
W	13.00	12.89	12.97	13.52
Au	16.76	18.67	16.09	–
Pb	14.54	14.54	14.37	13.64

The calculations are performed with the same effective threshold displacement energies E_d.

$E_d(\eta = 1)$ are shown in Table 2 for each measured value of the resistivity damage rate. The η values and $E_d(\eta = 1)$ values obtained for a same metal from the analysis of different experiments are rather in a good agreement. The exception is for titanium, nickel, niobium and silver, where there is a noticeable scattering of the data. For niobium and titanium the highest value of $\langle\eta\rangle$ ($\simeq$1.1) observed for the LHTL neutron irradiation [63] is not in an agreement with the other measurements. The same is for the lowest $\langle\eta\rangle$ value for nickel and silver ($\simeq$0.16) obtained from the data of Refs. [47,72].

For each metal from Table 2 the mean value of the defect production efficiency $\overline{\langle\eta\rangle}$ and threshold energy $\overline{E_d(\eta = 1)}$ has been calculated. The obtained mean values along with the statistical errors are shown in Table 4. It should be noted that the mean values of the efficiency and the threshold energy have the physical sense in case of the relative insensitivity of $\langle\eta\rangle$ and $E_d(\eta = 1)$ from the shape of the neutron irradiation spectrum (Section 5).

Table 4 shows that the maximal value of defect production efficiency is observed for titanium ($\langle\eta\rangle$ = 0.87), rhenium (0.87) and gallium (0.91) and the minimal $\langle\eta\rangle$ values is obtained for lead (0.1), potassium (0.065) and gadolinium (0.15). Unfortunately, at present, the uncertainty of the obtained $\langle\eta\rangle$ values cannot be evaluated precisely, because there is only single measurement of damage rate for each of these metals except titanium.

Table 4 shows the good agreement between the efficiency values for iron, nickel and stainless steel.

The mean efficiency value $\overline{\langle\eta\rangle}$ for *fcc* metals is equal to 0.34 ± 0.10, for *bcc* metals 0.54 ± 0.18 and for *hcp* metals 0.55 ± 0.28. For all metals the $\overline{\langle\eta\rangle}$ value is equal to 0.47 ± 0.21.

5. Calculation of defect production efficiency

5.1. The general dependence of defect production efficiency from the primary ion energy

The defect production efficiency in metals has been calculated by the method of molecular dynamics by many authors [8,14,57,78–94].

One should note the definite agreement between the results of the most of MD simulations. The typical dependence of η from the primary knock-on atom (PKA) energy obtained from the MD calculations [8,14,86,88] is shown in Fig. 4 for a number of metals. It is supposed that the E_{MD} energy [8,14,86,88] is equal approximately to T_{dam} in Eq. (2).

In the present work the MARLOWE code [6] based on the BCA approach [29,95–97] was applied for the calculation of the number of defects in irradiated materials. The parameters of the model [6] are chosen to get the agreement with the results of the defect production calculations by the MD method at the ion energies above 10 keV. The interatomic potential from Ref. [98] has been applied for iron, as in the MD simulation in Ref. [89]. For tungsten the interatomic potential from Ref. [99] has been used.

Fig. 5 shows the efficiency of defect production calculated by the MARLOWE code for iron and tungsten and the results of the MD calculations [14,86,88]. There is a substantial difference between the η values calculated by the BCA approach and the MD method at the energies below 10 keV. The binary collision approximation cannot reproduce the realistic dependence of η from the primary ion energies. In particular, it does not

Table 4
The mean values of the defect production efficiency and effective threshold energy obtained from the experimental damage resistivity rates at the temperatures $T = 4$–5 K

Metal	$\overline{\langle\eta\rangle}$	$\overline{E_d(\eta = 1)}$ (eV)
fcc		
Al	0.45 ± 0.07	61 ± 9
Ni	0.25 ± 0.06	142 ± 38
Cu	0.31 ± 0.03	99 ± 9
Pd	0.32 ± 0.03	129 ± 13
Ag	0.36 ± 0.11	124 ± 61
Pt	0.37 ± 0.06	123 ± 22
Au	0.43 ± 0.03	100 ± 7
Pb	0.10	247
bcc		
K	0.065	619
V	0.52 ± 0.04	111 ± 9
Fe	0.32 ± 0.05	129 ± 20
Nb	0.67 ± 0.21	124 ± 28
Mo	0.47 ± 0.07	141 ± 23
Ta	0.73 ± 0.09	125 ± 16
W	0.61 ± 0.08	150 ± 22
hcp		
Mg	0.45 ± 0.04	45 ± 4
Ti	0.87 ± 0.22	36 ± 8
Co	0.27 ± 0.06	138 ± 29
Zn	0.37	79
Zr	0.72 ± 0.13	57 ± 11
Cd	0.45	67
Gd	0.15	259
Re	0.87	69
Others		
Ga	0.91	13
Sn	0.79	28
Stainless steel	0.29	136

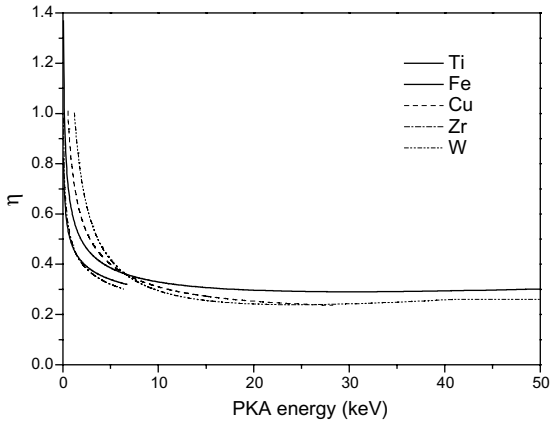

Fig. 4. The defect production efficiency obtained by the MD method for Ti [8], Fe [86,88], Cu [14], Zr [8] and W [14] plotted against the PKA energy. The E_d value is equal to 30 eV for Ti and Cu, 40 eV for Fe and 90 eV for W.

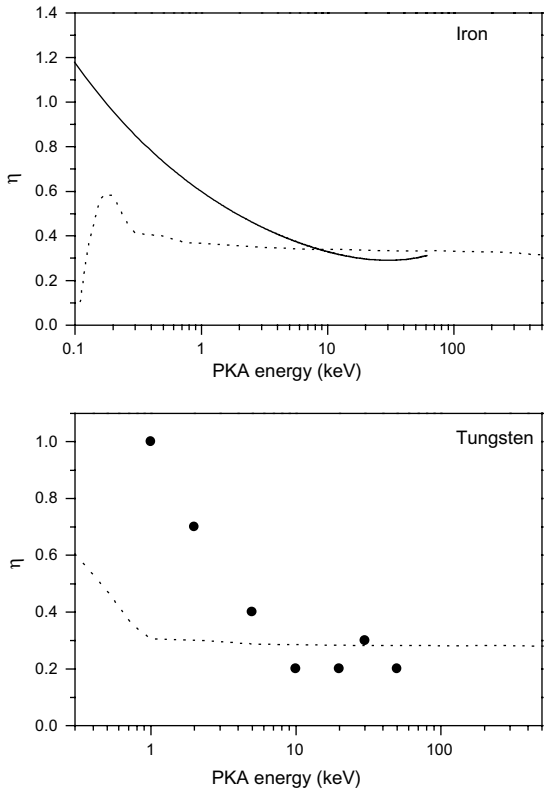

Fig. 5. The defect production efficiency calculated with the help of the MARLOWE code (dotted line) and obtained by the MD simulation for Fe [86,86] (solid line) and W [14] (full circles).

describe a few-body effect in a thermal spike phase, which plays a fundamental role in the defect production at energies above 250 eV.

5.2. The average efficiency of defect production in metals irradiated by neutrons with realistic spectra

The energy dependent η values calculated by the MD method in Refs. [8,14,86,88] were used for the calculation of the average defect production efficiency $\langle\eta\rangle$ in metals irradiated by neutrons of different energies.

The following functions were used for the efficiency calculation:

titanium [8]

$$\eta = 6.02E_{MD}^{0.786}/N_{NRT}, \quad E_{MD} \leqslant 5 \text{ keV}, \tag{9}$$

iron [86,88]:

$$\eta = 0.5608E_{MD}^{-0.3029} + 3.227 \times 10^{-3}E_{MD}, \quad E_{MD} \leqslant 40 \text{ keV}, \tag{10}$$

copper [14]:

$$\eta = 0.7066E_{\mathrm{MD}}^{-0.437} + 2.28 \times 10^{-3}E_{\mathrm{MD}}, \quad E_{\mathrm{MD}} \leqslant 20 \text{ keV}, \tag{11}$$

zirconium [8]:

$$\eta = 4.58E_{\mathrm{MD}}^{0.740}/N_{\mathrm{NRT}}, \quad E_{\mathrm{MD}} \leqslant 5 \text{ keV}, \tag{12}$$

tungsten [14]:

$$\eta = 1.0184E_{\mathrm{MD}}^{-0.667} + 5.06 \times 10^{-3}E_{\mathrm{MD}}, \quad E_{\mathrm{MD}} \leqslant 30 \text{ keV}, \tag{13}$$

where E_{MD} is the initial energy in the MD simulation taken in keV, $E_{\mathrm{MD}} \approx T_{\mathrm{dam}}$. It is supposed that the E_{d} value is equal to 30 eV for Cu and 90 eV for W.

The functions $\eta(E_{\mathrm{MD}})$ shown above correspond to the different temperatures adopted for the MD simulations. For titanium and zirconium, the temperature is equal to 100 K [8], for copper and tungsten – 10 K [14], for iron, the $\eta(E_{\mathrm{MD}})$ function relates to the temperature range from 100 to 900 K [86,88].

The energy dependent efficiencies, Eqs. (9)–(13) were introduced in the NJOY code [2] as a multiplication factors for the calculations based on the NRT model. At the energies above the limits shown in Eqs. (9)–(13) the constant efficiency values were assumed for the calculations. This approximation discussed in Refs. [14,86,88] is based on the idea of the subcascade formation at the high PKA energies. It is in agreement with the BCA calculations (Fig. 5). For copper at the energy E_{MD} below 0.45 keV and for tungsten below 1 keV, the efficiency was taken equal to unity according to Eqs. (11) and (13) due to the absence of more precise information.

The calculation of defect production efficiency $\langle\eta\rangle$ has been performed for neutron irradiation spectra from the following sources:

- TRIGA reactor (core),
- PWR reactor (core),
- Tight Lattice Light Water Reactor (TLLWR) (core),
- SNR-2 fast breeder reactor (core),
- TTB, FRM reactor [7],
- fission spectrum (Maxwellian, $\theta = 1.35$ MeV),
- HCPB fusion reactor (first wall) [100],
- 14.8 MeV neutrons,
- neutron spectrum from the Be(d,n) reaction induced by 40 MeV-deuterons [47].

The neutron spectra described above and normalized on the unity flux are plotted in Fig. 6. The detail view of the spectra in the energy range above 1 keV is given in Fig. 7.

Table 5 shows the averaged efficiency $\langle\eta\rangle$ calculated for titanium, iron, copper, zirconium and tungsten irradiated with neutrons of different sources. The data from ENDF/B-VI(8) were used for the calculations.

The comparison of the data from Table 5 shows that the average value of the efficiency for titanium, iron,

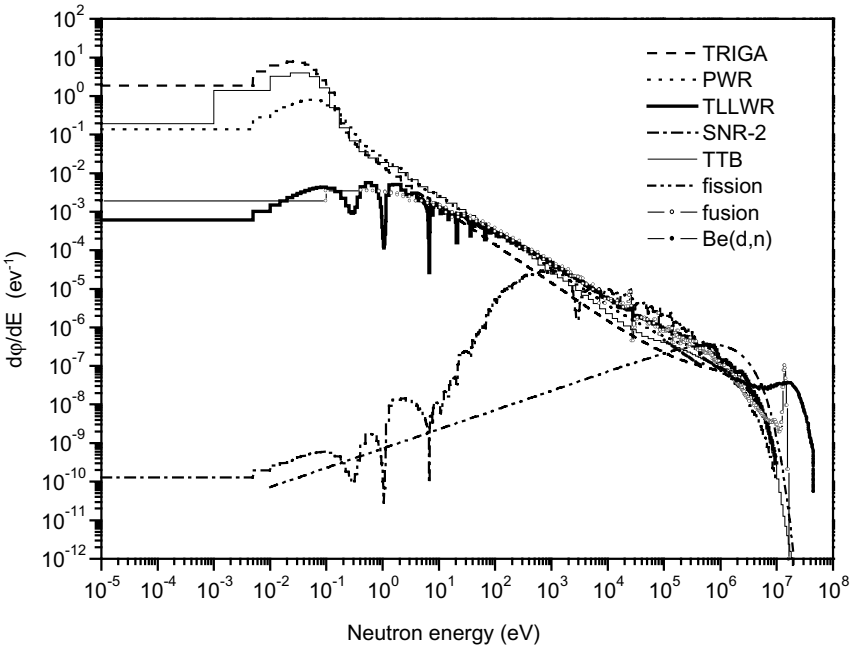

Fig. 6. Neutron spectra for various nuclear facilities.

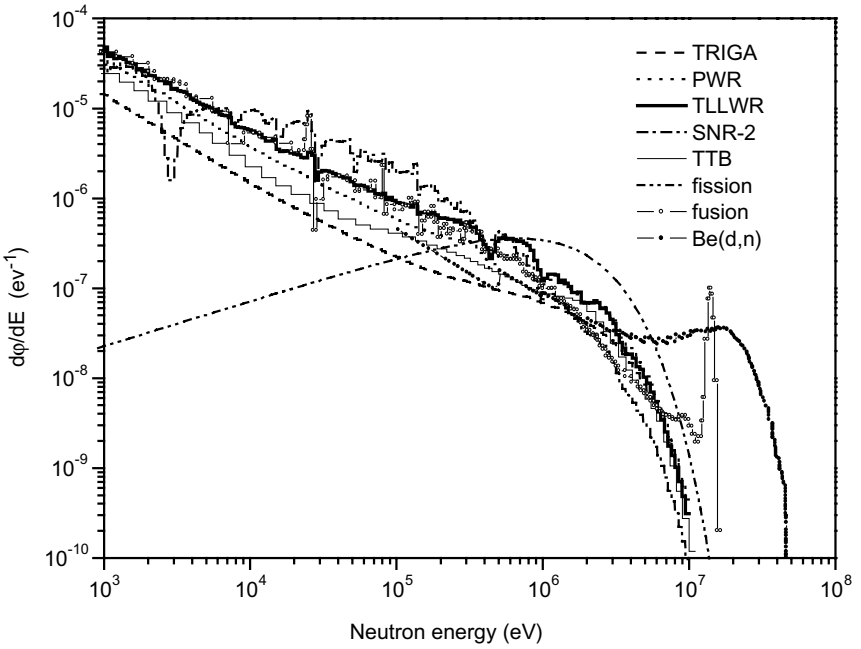

Fig. 7. Neutron spectra for various nuclear facilities at the energies above 1 keV.

Table 5
The averaged defect production efficiency $\langle\eta\rangle$ calculated for different neutron spectra

Source	Ti	Fe	Cu	Zr	W
TRIGA	0.34	0.33	0.29	0.31	0.34
PWR	0.33	0.32	0.27	0.31	0.35
TLLWR	0.34	0.32	0.28	0.31	0.37
SNR-2	0.36	0.34	0.33	0.33	0.47
TTB, FRM	0.34	0.33	0.28	0.31	0.35
Fission	0.32	0.31	0.25	0.30	0.31
Fusion reactor, first wall	0.33	0.32	0.26	0.31	0.31
14.8 MeV neutrons	0.32	0.31	0.24	0.30	0.27
Be(d,n), 40 MeV deuterons	–	0.31	0.24	–	0.27

copper and zirconium is rather independent of the shape of the nuclear spectrum. It gives an opportunity to predict realistic $\langle\sigma T_d\rangle$ values for these metals based on the mean values of $\langle\eta\rangle$ shown above and on the simple NRT calculations.

The value of defect production efficiency for tungsten is more sensitive to the type of the neutron irradiation spectrum. The maximum difference in the $\langle\eta\rangle$ value is for the Be(d,n) spectrum and 14.8 MeV neutrons (0.27) and the SNR-2 spectrum (0.47). The most sensitivity is shown by the radiative capture component of the damage comparing with the neutron elastic scattering.

With an increase of the contribution of high energy neutrons in the total flux the average efficiency value $\langle\eta\rangle$ decreases coming close to the asymptotic $\eta(T)$ value (Fig. 4). For this reason the lowest $\langle\eta\rangle$ values shown in Table 5 relate to the fission spectrum and the Be(d,n) spectrum. The highest $\langle\eta\rangle$ value is observed for the SNR-2 spectrum which has the lowest contribution of the energy range above 1 MeV in the total flux.

5.3. Comparison of the average defect production efficiency calculated with the help of the theoretical models and derived from the experimental dose rates

Comparison of the efficiency values $\langle\eta\rangle$ obtained with the help of the MD calculations (Table 5) with the efficiency derived from experimental damage rates (Tables 2 and 4) shows the good agreement for iron. The mean value $\overline{\langle\eta\rangle}$ obtained from Table 5 data (0.32 ± 0.1) is actually equal to the mean efficiency value derived from the experimental data (Table 4). This can be considered

as an indication of the weak temperature dependence of the defect production efficiency for iron discussed in Ref. [89].

There is good agreement in $\overline{\langle\eta\rangle}$ values for copper, $\overline{\langle\eta\rangle}$ (theory, Table 5) $= 0.27 \pm 0.03$ and $\overline{\langle\eta\rangle}$ (experiment, Table 4) $= 0.31 \pm 0.03$.

For titanium, zirconium and tungsten, the experimental $\overline{\langle\eta\rangle}$ values are 1.8–2.6 times higher than the theoretical efficiency values. It can be explained by the temperature dependence of the efficiency for titanium and zirconium. The same reduction of the η value was observed for copper at temperatures from 0 to 100 K in Ref. [101]. On the other hand, there is a strong dependence of the measured initial dose rate on the purity of zirconium and titanium [7], which complicates the interpretation of the difference between the theoretical and experimental efficiency values for these metals.

For tungsten, the difference between the experimental and theoretical $\langle\eta\rangle$ values has another origin. The comparison of the calculated and measured resistivity change for tungsten irradiated with high energy protons [14] shows the similar discrepancy between experimental data and the values obtained with the help of the efficiency η calculated by the MD method (Eq. (13), Fig. 4). The authors [14] have ascribed the discrepancy between experimental and theoretical resistivity change to the incorrect energy deposition calculation by the LAHET code.

In case of the neutron irradiation, the nuclear data from ENDF/B-VI(8) used for the recoil calculations for tungsten seem to be rather reliable. The use of other data libraries gives similar $\langle\sigma T_{\mathrm{d}}\rangle$ values (Table 3). For this reason the observed discrepancy between the theoretical and experimental $\langle\eta\rangle$ values for tungsten should be related to the problems of the measurement of the initial damage rate in Refs. [7,43,63,65] or to the MD calculations in Refs. [14,57]. Further studies are needed to understand the observed difference in the $\langle\eta\rangle$ values.

6. Conclusion

The available data of Frenkel pair resistivity ρ_{FP} were compiled and analyzed in the present work. The evaluated and recommended ρ_{FP} values were obtained for 22 metals and stainless steel (Table 1). The systematics of Frenkel pair resistivity has been constrained (Eq. (8)).

The experimental data of damage resistivity rates in metals were compiled and analyzed. The latest versions of nuclear data libraries ENDF/B-VI(8), JENDL-3.3, JEFF-3.0, BROND-2.2 and CENDL-2.1 were used for the averaged damage energy cross-section calculation.

The average defect production efficiency in metals $\langle\eta\rangle$ has been calculated for various neutron irradiation spectra (Tables 2 and 4).

The energy dependence of the defect production efficiency $\eta(E)$ has been calculated with the help of the BCA model and the MARLOWE code. The comparison with the result of the MD simulation shows the significant difference in the $\eta(E)$ values at the energies below 10 keV (Fig. 5).

The energy dependent efficiency values obtained by the MD method were used for the calculation of the average efficiency values $\langle\eta\rangle$ for the neutron spectra of the thermal reactor, the fast breeder reactor, the fusion facility and the Be(d,n) reaction. The comparison of the obtained $\langle\eta\rangle$ values with the efficiency values derived from experimental damage rates shows good agreement for iron and copper. For titanium, zirconium and tungsten the theoretical $\langle\eta\rangle$ values are about twice less than the experimental ones. In the case of titanium and zirconium the discrepancy in $\langle\eta\rangle$ values can be explained by the temperature dependence of the defect production efficiency. For tungsten the difference between the theoretical and experimental efficiency values may originate from the lack of the measurement routine as from the problems of the MD simulation.

Acknowledgements

The authors are greatly indebted to Dr L.R.Greenwood for the results of the SPECTER code calculations for the TTB, FRM neutron spectrum.

References

[1] M.J. Norgett, M.T. Robinson, I.M. Torrens, Nucl. Eng. Des. 33 (1975) 50.
[2] R.E. MacFarlane, NJOY99.0: Code System for Producing Pointwise and Multigroup Neutron and Photon Cross Sections from ENDF/B Data, RSICC Code Package PSR-480 (Report).
[3] J.S. Hendricks, G.W. McKinney, L.S. Waters, T.L. Roberts, et al. MCNPX, Version 2.5.d, Report LA-UR-03-5916, 2003.
[4] R.E. Prael, H. Lichtenstein, User Guide to LCS: The LAHET Code System, Report LA-UR-89-3014, 1989.
[5] L.R. Greenwood, R.K. Smither, SPECTER: neutron damage calculations for materials irradiations, Report ANL/FPP-TM-197, 1985.
[6] M.T. Robinson, MARLOWE: computer simulation of atomic collisions in crystalline solids (Version 15b), RSICC Code Package PSR-137 (Report).
[7] G. Wallner, M.S. Anand, L.R. Greenwood, M.A. Kirk, W. Mansel, W. Waschkowski, J. Nucl. Mater. 152 (1988) 146.
[8] D.J. Bacon, A.F. Calder, F. Gao, V.G. Kapinos, S.J. Wooding, Nucl. Instrum. and Meth. B 102 (1995) 37.
[9] P. Jung, Phys. Rev. B 23 (1981) 664.
[10] P. Jung, J. Nucl. Mater. 117 (1983) 70.
[11] J.W. Martin, J. Phys. F 2 (1972) 842.

[12] R.S. Averback, R. Benedek, K.L. Merkle, Phys. Rev. B 18 (1978) 4156.
[13] K.L. Merkle, W.E. King, A.C. Baily, K. Haga, M. Meshii, J. Nucl. Mater. 117 (1983) 4.
[14] M.J. Caturla, T. Diaz de la Rubia, M. Victoria, R.K. Corzine, M.R. James, G.A. Greene, J. Nucl. Mater. 296 (2001) 90.
[15] P. Ehrhart, W. Schilling, Phys. Rev. B 8 (1973) 2604.
[16] P. Ehrhart, H.G. Haubold, W. Schilling, Adv. Solid State Phys. 14 (1974) 87.
[17] J.B. Roberto, B. Schoenfeld, P. Ehrhart, Phys. Rev. B 18 (1978) 2591.
[18] P. Jung, Radiat. Eff. 51 (1980) 249.
[19] O. Dimitrov, C. Dimitrov, Radiat. Eff. 84 (1985) 117.
[20] G. Burger, H. Meissner, W. Schilling, Phys. Status Solidi 4 (1964) 281.
[21] J.A. Horak, T.H. Blewitt, Phys. Status Solidi 9 (1972) 721.
[22] P. Lucasson, in: M.T. Robinson, F.W. Young Jr. (Eds), Fundamental Aspects of Radiation Damage in Metals, vol. 1, 1976, p. 42 (CONF-75-1006-P1, US ERDA, Washington, DC, 1975).
[23] R.S. Averback, R. Benedek, K.L. Merkle, J. Sprinkle, L.J. Thompson, J. Nucl. Mater. 113 (1983) 211.
[24] O. Bender, P. Ehrhart, J. Phys. F: Metal Phys. 13 (1983) 911.
[25] R.S. Averback, T. Diaz de la Rubia, Solid State Phys. 51 (1997) 281.
[26] P. Jung, R.L. Chaplin, H.J. Fenzl, K. Reichelt, P. Wombacher, Phys. Rev. B 8 (1973) 553.
[27] P. Ehrhart, U. Schlagheck, J. Phys. F: Metal Phys. 4 (1974) 1575.
[28] W.E. King, R. Benedeck, K.L. Merkle, M. Meshii, in: J. Takamura, M. Doyama, M. Kiritani (Eds.), Point Defects and Defect Interactions in Metals, University of Tokyo, 1982, p. 789.
[29] M.T. Robinson, I.M. Torrens, Phys. Rev. B 9 (1974) 5008.
[30] R.E. Macfarlane, D.W. Muir. The NJOY Nuclear Data Processing System, Ver. 91, Report LA-12740 M, UC-413, 1994.
[31] M. Nakagawa, K. Böning, P. Rosner, G. Vogl, Phys. Rev. B 16 (1977) 5285.
[32] C.M. Jimenez, L.F. Lowe, E.A. Burke, C.H. Sherman, Phys. Rev. 153 (1967) 735.
[33] P.G. Lucasson, R.M. Walker, Phys. Rev. 127 (1962) 485.
[34] A. Sosin, Phys. Rev. 126 (1962) 1698.
[35] E.A. Burke, C.M. Jimenez, L.F. Lowe, Phys. Rev. 141 (1966) 629.
[36] J.S.N. Hancock, J.N. Lomer, cited by P.Vajda, Rev. Mod. Phys. 49 (1977) 481.
[37] P. Ehrhart, E. Segura, in: M.T. Robinson, F.W. Young Jr. (Eds.), Fundamental Aspects of Radiation Damage in Metals, vol. 1, 1976, p. 295 (CONF-75-1006-P1, US ERDA, Washington, DC, 1975).
[38] R.R. Coltman Jr., C.E. Klabunde, J.M. Williams, J. Nucl. Mater. 99 (1981) 284.
[39] W. Bauer, A. Sosin, Phys. Rev. 135 (1964) A521.
[40] W. Bauer, in: R.R. Hasiguti (Ed.), Lattice Defects and their Interactions, Gordon and Breach Science, New York, London, Paris, 1967, p. 567.
[41] R.O. Simmons, R.W. Baluffi, Phys. Rev. 129 (1963) 1533.
[42] B.S. Brown, T.H. Blewitt, T.L. Scott, A.C. Klank, J. Nucl. Mater. 52 (1974) 215.
[43] C.E. Klabunde, R.R. Coltman Jr., J. Nucl. Mater. 108&109 (1982) 183.
[44] F. Maury, M. Biget, P. Vajda, A. Lucasson, P. Lucasson, Phys. Rev. B 14 (1976) 5303.
[45] A. Iwase, S. Ishino, J. Nucl. Mater. 276 (2000) 178.
[46] P. Ehrhart, Mater. Res. Soc. Symp. 41 (1985) 13.
[47] M.A. Kirk, L.R. Greenwood, J. Nucl. Mater. 80 (1979) 159.
[48] P. Ehrhart, cited by O. Dimitrov, C. Dimitrov, Radiat. Eff. 84 (1985) 117.
[49] M. Biget, R. Rizk, P. Vajda, A. Besis, Solid State Commun. 16 (1975) 949.
[50] P. Vajda, M. Biget, Phys. Status Solidi A 23 (1974) 251.
[51] F. Maury, P. Vajda, M. Biget, A. Lucasson, P. Lucasson, Radiat. Eff. 25 (1975) 175.
[52] P. Ehrhart, J. Nucl. Mater. 69&70 (1978) 200.
[53] W. Schilling, J. Nucl. Mater. 69&70 (1978) 465.
[54] M. Hou, A. van Veen, L.M. Caspers, M.R. Yrma, Nucl. Instrum. and Meth 209&210 (1983) 19.
[55] P. Jung, W. Schilling, Phys. Rev. B 5 (1972) 2046.
[56] M. Biget, F. Maury, P. Vajda, A. Lucasson, P. Lucasson, Phys. Rev. B 19 (1979) 820.
[57] M.W. Guinan, J.H. Kinney, J. Nucl. Mater. 103&104 (1981) 1319.
[58] T.N. O'Neal, R.L. Chaplin, Phys. Rev. B 5 (1972) 3810.
[59] C.G. Shirley, R.L. Chaplin, Phys. Rev. B 5 (1972) 2027.
[60] P. Vajda, Rev. Mod. Phys. 49 (1977) 481.
[61] F. Maury, P. Vajda, A. Lucasson, P. Lucasson, Phys. Rev. B 8 (1973) 5496;
F. Maury, P. Vajda, A. Lucasson, P. Lucasson, Phys. Rev. B 8 (1973) 5506.
[62] P. Ehrhart, B. Schönfeld, Phys. Rev. B 19 (1979) 3896.
[63] S. Takamura, T. Aruga, K. Nakata, J. Nucl. Mater. 136 (1985) 159.
[64] S. Myhra, R.B. Gardiner, Radiat. Eff. 27 (1975) 35.
[65] M.W. Guinan, J.H. Kinney, J. Nucl. Mater. 108&109 (1982) 95.
[66] P. Ehrhart, B. Schönfeld, in: J. Takamura, M. Doyama, M. Kiritani (Eds.), Point Defects and Defect Interactions in Metals, University of Tokyo, 1982, p. 47.
[67] M. Biget, F. Maury, P. Vajda, A. Lucasson, P. Lucasson, Radiat. Eff. 7 (1971) 223.
[68] J. McIlwain, R. Gardiner, A. Sosin, S. Myhra, Radiat. Eff. 24 (1975) 19.
[69] E.A. Brandes, G.B. Brook (Eds.), Smithels Metals Reference Book, Butterworth Heinemann, 7th Ed., 1992 (Chapter 19).
[70] I.S. Grigor'ev, E.Z. Meilikhov (Eds.), Fizicheskie Velichini, Reference Book, Energoatomizdat, Moscow, 1991.
[71] C. Kittel, Introduction to Solid State Physics, John Wiley, New York, 1986.
[72] R.C. Birtcher, R.S. Averback, T.H. Blewitt, J. Nucl. Mater. 75 (1978) 167.
[73] F. Rullier-Albenque, H. Bielska-Lewandowska, Y. Quere, G. Wallner, P. Müller, J. Nucl. Mater. 151 (1988) 251.
[74] M. Nakagawa, W. Mansel, K. Böning, P. Rosner, G. Vogl, Phys. Rev. B 19 (1979) 742.
[75] G. Wallner, K. Böning, U. Dedek, J. Phys. F 16 (1986) 257.

[76] D.E. Cullen, PREPRO 2002, ENDF/B Pre-processing Codes, GROUPIE, Report IAEA-NDS-39, February 5, 2003. Available from <http://www.llnl.gov/cullen1/>.
[77] L.R. Greenwood, private communication.
[78] Horngming Hsieh, T. Diaz de la Rubia, R.S. Averback, Phys. Rev. B 40 (1989) 9986.
[79] T. Diaz de la Rubia, W.J. Phythian, J. Nucl. Mater. 191–194 (1992) 108.
[80] A.J.E. Foreman, W.J. Phythian, C.A. English, Philos. Mag. A 66 (1992) 671.
[81] D.J. Bacon, T. Diaz de la Rubia, J. Nucl. Mater. 216 (1994) 275.
[82] W.J. Phythian, R.E. Stoller, A.J.E. Foreman, A.F. Calder, D.J. Bacon, J. Nucl. Mater. 223 (1995) 245.
[83] R.E. Stoller, J. Nucl. Mater. 233–237 (1996) 999.
[84] R.E. Stoller, G.R. Odette, B.D. Wirth, J. Nucl. Mater. 251 (1997) 49.
[85] N. Soneda, T. Diaz de la Rubia, Philos. Mag. A 78 (1998) 995.
[86] R.E. Stoller, L.R. Greenwood, J. Nucl. Mater. 271&272 (1999) 57.
[87] M.J. Caturla, N. Soneda, E. Alonso, B.D. Wirth, T. Diaz de la Rubia, J.M. Perlado, J. Nucl. Mater. 276 (2000) 13.
[88] R.E. Stoller, Nucl. Eng. Des. 195 (2000) 129.
[89] R.E. Stoller, J. Nucl. Mater. 276 (2000) 22.
[90] E. Alonso, M.J. Caturla, T. Diaz de la Rubia, J.M. Perlado, J. Nucl. Mater. 276 (2000) 221.
[91] N.V. Doan, J. Nucl. Mater. 283–287 (2000) 763.
[92] R.E. Stoller, J. Nucl. Mater. 307–311 (2002) 935.
[93] Yu.N. Osetsky, D.J. Bacon, B.N. Singh, J. Nucl. Mater. 307–311 (2002) 866.
[94] F. Gao, D.J. Bacon, P.E.J. Flewitt, T.A. Lewis, J. Nucl. Mater. 249 (1997) 77.
[95] M.T. Robinson, Phys. Rev. B 40 (1989) 10717.
[96] M.T. Robinson, J. Nucl. Mater. 216 (1994) 1.
[97] M.T. Robinson, Radiat. Eff. 141 (1997) 1.
[98] A.F. Calder, D.J. Bacon, J. Nucl. Mater. 207 (1993) 25.
[99] J.F. Ziegler, J.P. Biersack, U. Littmark, Stopping Powers and Ranges of Ions in Matter, Pergamon, New York, 1985.
[100] Y. Chen, U. Fischer, P. Pereslavtsev, F. Wasastjerna, The EU Power Plant Conceptual Study – Neutronic Design Analyses for Near Term and Advanced Reactor Models, Report FZKA 6763, 2003.
[101] S.J. Zinkle, B.N. Singh, J. Nucl. Mater. 199 (1993) 173.
[102] P. Jung, in: H. Ullmaier (Ed.), Production of Atomic Defects in Metals, Landolt-Börnstein, Group III: Crystal and Solid State Physics, Springer-Verlag, Berlin, vol. 25, 1991, p. 1.
[103] G.W. Iseler, H.I. Dawson, A.S. Mehner, J.W. Kauffman, Phys. Rev. 146 (1966) 468.
[104] H.H. Neely, W. Bauer, Phys. Rev. 149 (1966) 535.
[105] H.M. Simpson, R.L. Chaplin, Phys. Rev. 185 (1969) 958.
[106] H.G. Haubold, D. Martinsen, J. Nucl. Mater. 69&70 (1978) 644.
[107] D.N. Borton, A.E. Mardiguian, H.B. Huntington, G.L. Salinger, Bull. Am. Phys. Soc. 19 (II) (1974) 257 (CI9).
[108] R.L. Chaplin, K. Sonnenberg, R.R. Coltman Jr., Radiat. Eff. 27 (1975) 119.
[109] M. Biget, F. Maury, P. Vajda, A. Lucasson, P. Lucasson, J. de Phys. 40 (1979) 293.
[110] M. Biget, P. Vajda, F. Maury, A. Lucasson, P. Lucasson, in: M.T. Robinson, F.W. Young Jr. (Eds.) Fundamental Aspects of Radiation Damage in Metals, 1976, p. 66 (CONF-75-1006-P1, US ERDA, Washington, DC, 1975).
[111] R. Rizk, P. Vajda, A. Lucasson, P. Lucasson, Phys. Status Solidi A 18 (1973) 241.
[112] F. Maury, M. Biget, P. Vajda, A. Lucasson, P. Lucasson, Radiat. Eff. 38 (1978) 53.
[113] H. Kugler, PhD thesis, University of Stuttgart, 1980, cited by P. Jung, in: H. Ullmaier (Ed.), Production of Atomic Defects in Metals, Landolt-Börnstein, Group III: Crystal and Solid State Physics, Springer-Verlag, Berlin, vol. 25, 1991, p. 1.
[114] W.E. Faust, T.N. O'Neal, R.L. Chaplin, Phys. Rev. 183 (1969) 609.
[115] F. Maury, A. Lucasson, P. Lucasson, Crystal Lattice Defects 2 (1971) 47.
[116] S. Myhra, R.B. Gardiner, Radiat. Eff. 18 (1973) 39.
[117] J.N. Daou, J.E. Bonnet, P. Vajda, M. Biget, A. Lucasson, P. Lucasson, Phys. Status Solidi A 40 (1977) 101.
[118] J.N. Daou, E.B. Hannech, P. Vajda, M. Biget, A. Lucasson, P. Lucasson, Philos. Mag. A 41 (1980) 225.
[119] H. Vandenborre, L. Stals, J. Cornelis, J. Nihoul, Radiat. Eff. 21 (1974) 137.
[120] G. Quelard, J. Dural, J. Ardonceau, D. Lesueur, Radiat. Eff. 39 (1978) 45.
[121] J.N. Daou, P. Vajda, A. Lucasson, P. Lucasson, Radiat. Eff. 61 (1982) 93.
[122] A. Dunlop, M.H. Gely, Radiat. Eff. 79 (1983) 159.
[123] J.N. Daou, P. Vajda, A. Lucasson, P. Lucasson, Radiat. Eff. 84 (1985) 211.
[124] J.N. Daou, P. Vajda, A. Lucasson, P. Lucasson, J.P. Burger, Phys. Lett. 107A (1985) 142.
[125] J.N. Daou, P. Vajda, A. Lucasson, P. Lucasson, J. Phys. F: Metal Phys. 10 (1980) 583.
[126] C. Weinberg, Y. Quere, Mater. Sci. Forum 15–18 (1987) 943.